Impact of Polarization-Mode Dispersion on Measurement of Zero-Dispersion Wavelength Through Four-Wave Mixing

Q. Lin and Govind P. Agrawal

***Abstract*—We develop a vector theory of four-wave mixing and use it to discuss the impact of polarization-mode dispersion (PMD) on measurements of the variations of the zero-dispersion wavelength along an optical fiber. We show that the PMD induces large fluctuations in the idler power and affects considerably the accuracy of such measurements.**

***Index Terms*—Fiber dispersion, four-wave mixing (FWM), polarization-mode dispersion (PMD), zero-dispersion wavelength (ZDWL).**

CHROMATIC dispersion (CD) of any optical fiber, although designed to be norminally constant, varies along its length because of unavoidable variations in the core diameter. Several nondestructive measurement techniques make use of four-wave mixing (FWM) occurring inside optical fibers [1]–[5]. As FWM is sensitive to the local value of the zero-dispersion wavelength (ZDWL), or the CD, it provides an efficient way to map ZDWL/CD variations along the fiber length. However, FWM is sensitive not only to the phase mismatch between the pump, signal, and idler waves but also to their relative polarization orientations [6]. Residual birefringence inside optical fibers induces polarization-mode dispersion (PMD) and randomizes the state of polarization (SOP) of any optical wave [7]. The random nature of PMD would induce fluctuations in the idler power generated through the FWM process. Such PMD-induced power fluctuation would affect the mapping of ZDWL or CD whenever FWM is used. In this letter, we present a vector theory of FWM by including the PMD-induced random change in the SOPs of the three waves. We use this theory to show that PMD induces considerable fluctuations in the idler power during ZDWL/CD mapping and discuss its impact on the measurement accuracy.

By using the nonlinear polarization for silica glass [6] and introducing the Jones vectors $|A_p\rangle$, $|A_s\rangle$, and $|A_i\rangle$, associated with the pump, signal, and idler waves, we obtain the following three vector equations governing the degenerate FWM process in optical fibers in which two pump photons mix to create a pair of signal and idler photons such that $2\omega_p \rightarrow \omega_s + \omega_i$

$$\frac{d|A_p\rangle}{dz} = -\frac{\alpha}{2}|A_p\rangle + i\left(k_p - \frac{1}{2}\omega_p\vec{\beta}\cdot\vec{\sigma}\right)|A_p\rangle \tag{1}$$

$$\frac{d|A_s\rangle}{dz} = -\frac{\alpha}{2}|A_s\rangle + i\left(k_s - \frac{1}{2}\omega_s\vec{\beta}\cdot\vec{\sigma}\right)|A_s\rangle \tag{2}$$

$$\frac{d|A_i\rangle}{dz} = -\frac{\alpha}{2}|A_i\rangle + i\left(k_i - \frac{1}{2}\omega_i\vec{\beta}\cdot\vec{\sigma}\right)|A_i\rangle + \frac{i\gamma}{3}\left[2|A_p\rangle\langle A_p^*| + \langle A_p^*|A_p\rangle\right]|A_s^*\rangle \tag{3}$$

where ω_j and $k_j (j = p, s, i)$ are optical frequencies and propagation constants for the pump, signal, and idler waves, respectively. The idler is sometimes called the Stokes or anti-Stokes wave depending on whether it occurs on the red or blue side of the pump [2]. The location of the three waves can be close to [3] or far from [2] the ZDWL depending on whether ZDWL or CD needs to be mapped. In this letter, we choose them close to ZDWL and focus mainly on the ZDWL mapping. In (1)–(3), $\gamma = n_2\omega_p/cA_{\text{eff}}$ is the nonlinear parameter, A_{eff} is the effective core area [6], and α accounts for fiber losses. The three components of $\vec{\sigma}$ represent the Pauli matrices [6], [7]. We neglected pump depletion and signal amplification because both the pump and signal powers are much larger than the idler power in practice. Moreover, these two powers are either not large enough [1], [3], [5] or adjusted (signal power twice the copolarized pump power) such that the phase mismatch induced by self-phase and cross-phase modulations is cancelled automatically [2], [4]. For this reason, we neglect their effects in this letter.

The vector $\vec{\beta}$ governs the birefringence-induced fast SOP variations. What matters in the FWM process is the relative orientations of the signal and idler's SOPs with respect to the pump. It is, thus, convenient to work in a rotating frame in which the pump SOP remains fixed. Making a further transformation $|A\rangle \rightarrow |A\rangle\exp\{\int_0^z ik_p dz\}$, (1) contains only the loss term and can be easily integrated. Equations (2) and (3) take the following form in the rotating frame:

$$\frac{d|A_s\rangle}{dz} = -\frac{\alpha}{2}|A_s\rangle + i\left(\Delta k_s - \frac{1}{2}\Delta\omega\vec{b}\cdot\vec{\sigma}\right)|A_s\rangle \tag{4}$$

$$\frac{d|A_i\rangle}{dz} = -\frac{\alpha}{2}|A_i\rangle + i\left(\Delta k_i + \frac{1}{2}\Delta\omega\vec{b}\cdot\vec{\sigma}\right)|A_i\rangle + i\varepsilon\langle A_s|A_p\rangle|A_p\rangle \tag{5}$$

where $\Delta k_j = k_j - k_p, (j = s, i)$, $\Delta\omega = \omega_s - \omega_p$, and $\varepsilon = 8\gamma/9$. The vector $\vec{b}$ is related to $\vec{\beta}$ by a rotation and is responsible for PMD. As the fiber length is typically much longer than the birefringence correlation length, we model $\vec{b}$ as a three-dimensional

Manuscript received November 11, 2002; revised July 15, 2003. This work was supported by the National Science Foundation under Grant ECS-9903580 and Grant ECS-0320816.

The authors are with the Institute of Optics, University of Rochester, Rochester, NY 14627 USA (e-mail: linq@optics.rochester.edu).

Digital Object Identifier 10.1109/LPT.2003.819727

stochastic process whose first- and second-order moments are given by

$$\left\langle \vec{b}(z) \right\rangle = 0, \quad \left\langle \vec{b}(z_1)\vec{b}(z_2) \right\rangle = \frac{1}{3} D_p^2 \overleftrightarrow{I}\, \delta(z_2 - z_1) \tag{6}$$

where $\overleftrightarrow{I}$ is the second-order unit tensor, and D_p is the PMD parameter.

Equations (4) and (5) show that fast polarization changes induced by residual birefringence reduce the FWM efficiency by a factor of 8/9 [8], [9]. In the absence of birefringence, the FWM process is quite different for different pump polarizations due to the requirement of angular momentum conservation. However, in the presence of birefringence, the FWM process depends on the inner product $\langle A_s | A_p \rangle$. As a result, the FWM process depends only on the relative orientation between the pump and signal SOPs.

What is important to know is the evolution of the idler power $D_0 \equiv \langle A_i | A_i \rangle$ along the fiber, which is found, from (4) and (5), to relate to the signal Stokes vector $\vec{S} \equiv \langle A_s | \vec{\sigma} | A_s \rangle$, signal power $S_0 = |\vec{S}|$, and two complex quantities $\rho \equiv i\langle A_s | A_i^* \rangle$ and $\vec{\Gamma} \equiv i\langle A_s | \vec{\sigma} | A_i^* \rangle$. After averaging the dynamic equation of D_0 over the birefringence fluctuations, we obtain the following coupled but deterministic equations in the case of a linearly polarized pump along the x axis in the Stokes space [10]:

$$\frac{d\langle D_0 \rangle}{dz} = -\alpha \langle D_0 \rangle + \varepsilon P_0 Re(U) \tag{7}$$

$$\frac{dU}{dz} = -\left(\alpha + i\kappa + \frac{\eta}{2}\right) U + \varepsilon P_0 \left(S_0 + \langle S_x \rangle\right) \tag{8}$$

$$\frac{d\langle S_x \rangle}{dz} = -(\alpha + \eta)\langle S_x \rangle \tag{9}$$

where $U = \langle \rho \rangle + \langle \Gamma_x \rangle$, $\kappa = k_s + k_i - 2k_p$, $\eta = D_p^2(\Delta\omega)^2/3$, and $P_0(z)$ is the pump power. When the input signal is copolarized with the pump, the analytic solution is given by

$$\langle D_0(L) \rangle = 2\varepsilon^2 P_0^2(0) S_0(0) e^{-\alpha z} \int_0^z dz_1 e^{-\left(\alpha + \frac{\eta}{2}\right) z_1} \times \int_0^{z_1} dz_2 \cosh\left(\frac{\eta z_2}{2}\right) e^{-\alpha z_2} \cos\left(\int_{z_2}^{z_1} dz_3 \kappa(z_3)\right). \tag{10}$$

If the fiber has no birefringence, $\eta = 0$ and $\varepsilon = \gamma$, then (10) returns to the deterministic case and coincides with the results of [3].

For the dispersion-measurement problem, we need to focus on the PMD-induced fluctuations in the idler power. The relative level of such fluctuations can be obtained from (4) and (5) using

$$\sigma_i^2 = \frac{\left\langle D_0^2(L) \right\rangle - \langle D_0(L) \rangle^2}{\langle D_0(L) \rangle^2}. \tag{11}$$

The calculation of σ_i^2 requires the second-order moment $\langle D_0^2(L) \rangle$ of the idler, which is related to the second-order moments of $\vec{S}$, D_0, ρ, $\vec{\Gamma}$, and their combinations. Following the same procedure described earlier, we obtain the equations governing the evolution of these second-order moments and solve them numerically.

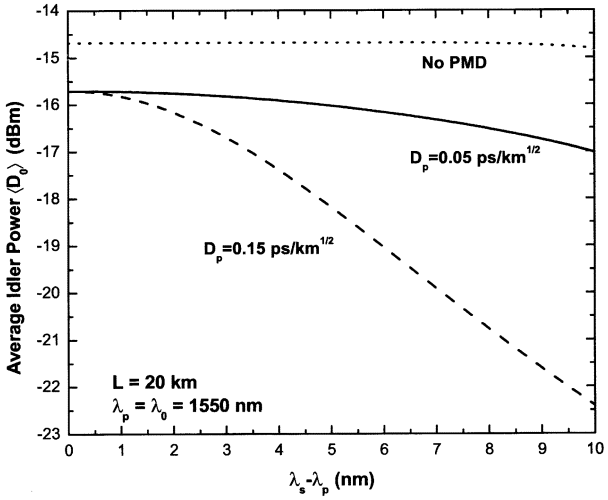

Fig. 1. Average idler power as a function of wavelength detuning between the signal and the pump for two values of the PMD parameter. The dotted line shows the case without birefringence. Other parameters are given in the text.

Fig. 1 shows the average idler power as a function of wavelength detuning between the signal and the pump for two D_p values when the input signal is copolarized with the pump. The pump wavelength λ_p is located at the fixed ZDWL of $\lambda_0 = 1550$ nm so that the idler power is maximized and its spectrum is flat in a wide range of detuning in the case absent of residual birefringence (dotted line). In general, λ_p does not have to coincide with λ_0 but should be close to it to maintain a high FWM conversion efficiency [3]. We used $\gamma = 2\ \mathrm{W}^{-1}/\mathrm{km}$, $L = 20$ km, $\beta_3 = 0.1\ \mathrm{ps}^3/\mathrm{km}$, $\beta_4 = 1.0 \times 10^{-4}\ \mathrm{ps}^4/\mathrm{km}$, $\alpha = 0.2$ dB/km, and $P_0(0) = S_0(0) = 5$ mW. When the signal wavelength is close to the pump, the idler power is proportional to $(8\gamma/9)^2$, and residual birefringence reduces the idler power by about $20\log_{10}(9/8) \approx 1$ dB. When the signal wavelength deviates considerably from the pump, the PMD effects increase, and the idler power decreases. The larger D_p, the larger the drop in the idler power.

Fig. 2 shows the fluctuation level of idler power corresponding to the case of Fig. 1. Fluctuations increase quickly when the signal wavelength is detuned away from the pump. Idler fluctuations can be as large as 17% when $\lambda_s - \lambda_p = 10$ nm even for $D_p = 0.05\ \mathrm{ps}/\sqrt{\mathrm{km}}$. Fluctuations increase drastically with D_p. When $D_p = 0.15\ \mathrm{ps}/\sqrt{\mathrm{km}}$, fluctuations become 57% for the same detuning. The curves similar to those shown in Figs. 1 and 2 are obtained when D_p changes because the PMD effects are determined by $D_p^2(\Delta\omega)^2$. When FWM is used for ZDWL mapping, the spatial resolution depends on the wavelength difference between the signal and the pump; the larger the difference, the higher the resolution [3]. However, as seen in Figs. 1 and 2, the PMD effects increase quickly with the wavelength difference and would reduce the accuracy of ZDWL mapping. One, thus, needs to be careful to balance the resolution and accuracy.

Figs. 3 and 4 show the idler spectrum and its fluctuations when pump wavelength is varied. The detuning between the signal and the pump $\lambda_s - \lambda_p$ is fixed to 3 nm. Other parameters are the same as Fig. 1. The dotted line shows the case absent of residual birefringence; the thick and thin lines show the cases of $D_p = 0.05$ and $0.15\ \mathrm{ps}/\sqrt{\mathrm{km}}$, respectively. The PMD ef-

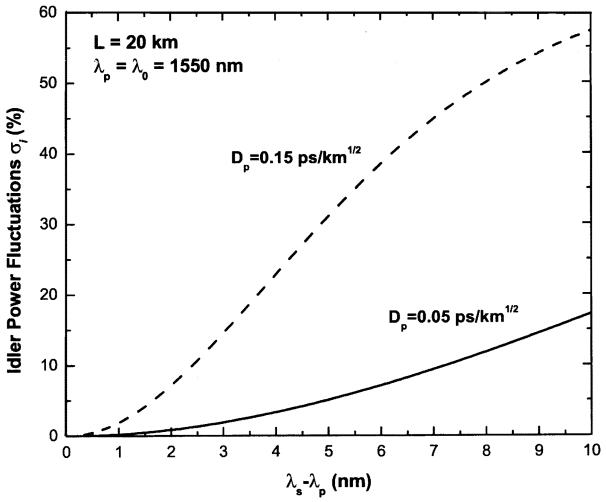

Fig. 2. Fluctuation levels of idler power as a function of wavelength detuning between the signal and the pump for two values of the PMD parameter. Other parameters are the same as in Fig. 1.

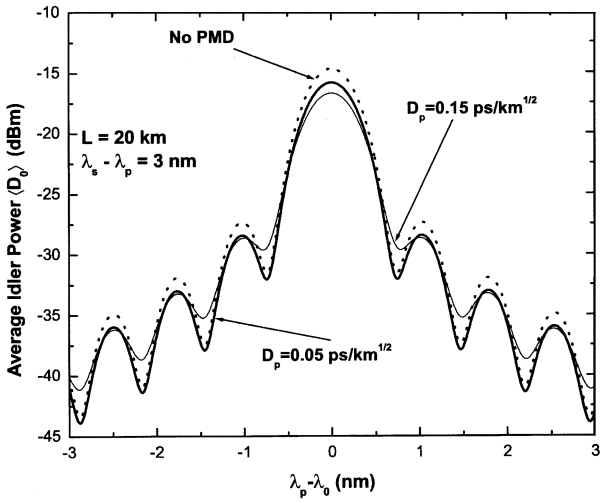

Fig. 3. Average idler power as a function of pump wavelength detuning from the ZDWL for two values of the PMD parameter. The dotted line shows the case without birefringence. Other parameters are the same as in Fig. 1.

fects smooth the oscillation structure in the idler spectrum that is important to provide the information on ZDWL [3]. More importantly, large amount of fluctuations appear even for the small detuning of 3 nm. When $D_p = 0.15$ ps/$\sqrt{\text{km}}$, fluctuations in the range of 25% to 49% are expected. The pump-scanned idler spectrum is commonly used in ZDWL mapping [1], [3], [5]. All the fine structure in the spectrum is interpreted as information associated with local variations of the ZDWL. Clearly, one should be careful when interpreting such spectra because large fluctuations induced by PMD might be included [3]. Since PMD effects changes with time, long-term repeated measurements may be required to obtain the average spectrum. Equation (10) should be used to interpret the data.

Apart from the pump-scanned idler spectrum, the oscillation periods of the idler power along the fiber can be used to map the CD directly when the pump and signal work far away from the ZDWL [2], [4]. However, PMD would induce extra phase mismatch and, thus, change the local oscillation period randomly [11]. The whole theory presented above can also be applied to

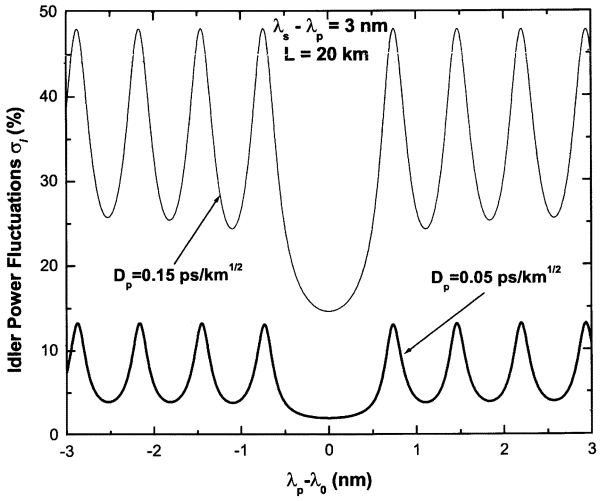

Fig. 4. Fluctuation levels of idler power as a function of the pump wavelength detuning from the ZDWL under conditions of Fig. 1.

discuss the PMD effects on the CD measurements if one includes the effects of the finite pump and signal pulsewidths and the Rayleigh backscattered nature of the idler.

In summary, we have developed a general vector theory to include the PMD effects occurring inside optical fibers during the FWM process. We found that PMD changes the average idler power significantly and introduces a large amount of fluctuations depending on the value of the PMD parameter. In measurements based on the pump-scanned idler spectrum or the spatial oscillation periods, PMD induces large fluctuations and would reduce the measurement accuracy. Long-term repeated measurement might be necessary for the dispersion mapping to reduce the PMD effects.

REFERENCES

[1] H. Onaka, K. Otsuka, H. Miyata, and T. Chikama, "Measuring the longitudinal distribution of four-wave mixing efficiency in dispersion-shifted fibers," *IEEE Photon. Technol. Lett.*, vol. 6, pp. 1454–1456, Dec. 1994.

[2] L. F. Mollenauer, P. V. Mamyshev, and M. J. Neubelt, "Method for facile and accurate measurement of optical fiber dispersion maps," *Opt. Lett.*, vol. 21, pp. 1724–1726, 1996.

[3] I. Brener, P. P. Mitra, D. D. Lee, and D. J. Thomson, "High-resolution zero-dispersion wavelength mapping in single-mode fiber," *Opt. Lett.*, vol. 23, pp. 1520–1522, 1998.

[4] J. Gripp and L. F. Mollenauer, "Enhanced range for OTDR-like dispersion map measurement," *Opt. Lett.*, vol. 23, pp. 1603–1605, 1998.

[5] M. González-Herráez, P. Corredera, M. L. Hernanz, and J. A. Méndez, "Retrieval of the zero-dispersion wavelength map of an optical fiber from measurement of its continuous-wave four-wave mixing efficiency," *Opt. Lett.*, vol. 27, pp. 1546–1548, 2002.

[6] G. P. Agrawal, *Nonlinear Fiber Optics*, 3rd ed. New York: Academic, 2001.

[7] H. Kogelnik, R. M. Jopson, and L. E. Nelson, *Optical Fiber Telecommunications IV B*, I. P. Kaminow and T. Li, Eds. San Diego, CA: Academic, 2002, ch. 15.

[8] P. K. Wai, C. R. Menyuk, and H. H. Chen, "Stability of solitons in randomly varying birefringence," *Opt. Lett.*, vol. 16, pp. 1231–1233, 1991.

[9] S. G. Evangelides Jr., L. F. Mollenauer, J. P. Gordon, and N. S. Bergano, "Polarization multiplexing with solitons," *J. Lightwave Technol.*, vol. 10, pp. 28–35, Jan. 1992.

[10] C. W. Gardiner, *Handbook of Stochastic Methods*, 2nd ed. New York: Springer-Verlag, 1985.

[11] C. Vinegoni, H. Chen, M. Leblanc, G. W. Schinn, M. Wegmuller, and N. Gisin, "Distributed measurement of chromatic dispersion and nonlinear coefficient in low-PMD dispersion-shifted fibers," *IEEE Photon. Technol. Lett.*, vol. 15, pp. 739–741, May 2003.